A Noninvasive Cross-Correlation Ultrasound Technique for Detecting Spatial Profile of Laser-Induced Coagulation Damage —An *In Vitro* Study

Zhigang Sun, Hao Ying*, *Senior Member, IEEE*, and Jialiang Lu, *Member, IEEE*

***Abstract*—A cross-correlation A-mode ultrasound technique is proposed for noninvasively detecting the spatial profile of coagulation damage in tissue being irradiated by laser. The basic assumption underlying this technique is that when coagulation is taking place in a tissue region, owing to thermally-induced structure changes in tissue, the waveform of echo signal scattered from that region should be changing accordingly. Our technique consists of four steps: 1) repeatedly sending the same acoustic signal to the tissue being heated; 2) tracking echo signals scattered from many small tissue regions using a cross-correlation echo-tracking technique; 3) quantifying waveform change of echo signal scattered from each region by means of cross-correlation coefficient between the currently acquired signal and a reference signal; 4) using the spatial profile of the degree of the waveform change to represent the tissue coagulation status at different depths. We carried out 23 heating experiments on fresh canine liver samples using a Nd : YAG laser (1064 nm wavelength) at various light intensity (62 to 105 W/cm^2) and exposure time (20 to 350 s). A 13-mm-diameter 10-MHz broadband single-element spherical focused ultrasound transducer was used. The spatial profiles of the degree of coagulation damage in the heated tissues, as determined by our technique, qualitatively agreed with the grossly inspected results. They also appeared to be consistent with the experimental and theoretical findings in the literature on laser-tissue interaction. Moreover, we developed an automatic procedure to compute the coagulation depth using the spatial profiles of the waveform change. We used the result as an indirect but quantitative means for evaluating the technique. Good overall agreement with a root mean square (rms) difference of only 0.81 mm was obtained between the computed and visually inspected final coagulation depths for the 23 experiments.**

***Index Terms*—Coagulation, cross correlation, echo-tracking, lasers, thermal therapy, ultrasound.**

I. Introduction

LASER thermal therapies have been widely explored [1]. The transport and deposition of heat in tissue is a complex process involving conduction, convection, radiation, metabolism, evaporation and physical phase change. Depending on the degree of temperature rise and its history, optical-thermal response of tissue may be classified into three categories. They are 1) tissue hyperthermia that takes place at 43 °C–50 °C and causes cell death, 2) tissue coagulation that starts at about 55 °C and leads to protein denaturation, and 3) tissue vaporization, charring, and ablation at 100 °C or above [2]. The selection of treatment parameters, such as heating rate and duration, dramatically influences the overall tissue response. To effectively treat lesions without damaging the surrounding normal tissue, techniques that could monitor the thermal activities inside the tissue are highly desirable.

Noninvasive assessment of the extent of thermal coagulation in tissue has been investigated by many researchers. Some of the researches have been discussed briefly in [3]. Most of the existing work is either qualitative or required off-line manual/interactive image analysis with involvement of human beings to gain quantitative estimation. Recently, we have developed an ultrasound technique for noninvasively and automatically determining the progress of tissue coagulation front in real-time [3]. Nevertheless, at present there exists no technique in the literature that is capable of detecting the spatial profile of the degree of coagulation damage during heating.

The purpose of this paper is to establish the feasibility of a novel cross-correlation technique for noninvasively detecting the spatial profile of the degree of coagulation damage along the diagnostic ultrasound beam axis in the tissue being heated. This study is an extension of our earlier work [3], which only detects coagulation boundary. The basic idea underlying the technique is that the more the tissue structure in a region has been altered by the heating (e.g., tissue denaturation), the more the ultrasound signal scattered from that region should change. Hence the degree of signal waveform change could be used to infer the degree of tissue structure change. Our technique includes two key components. One is to track echo signals scattered from predetermined small tissue regions in the course of heating using a cross-correlation technique. The other is to quantitatively measure the degree of waveform change of the tracked echo signals with respect to a reference signal acquired at a selected moment in the beginning stage of the heating.

II. Experimental Setup and Procedure

The experimental setup is depicted in Fig. 1. Fresh canine liver sample harvested immediately after animal sacrifice was placed on an 8-mm-thick Plexiglas plate and immersed in a glass tank ($L \times W \times H = 50 \times 25 \times 30$ cm^3) filled with 23 °C tap or

Manuscript received November 10, 1998; revised October 2, 2000. The work of H. Ying was supported in part by a Biomedical Engineering Research grant from the Whitaker Foundation and by a grant from The Advance Technology Program of Texas Higher Education Coordinating Board. *Asterisk indicates corresponding author.*

Z. Sun is with the Industrial Materials Institute of the National Research Council Canada.

*H. Ying is with the Electrical and Computer Engineering Department, Wayne State University, Detroit, MI 48202 USA (e-mail: hying@ece.wayne.edu).

J. Lu is with Hallibunon Corporation, Houston, TX 77204 USA.

Publisher Item Identifier S 0018-9294(01)00573-0.

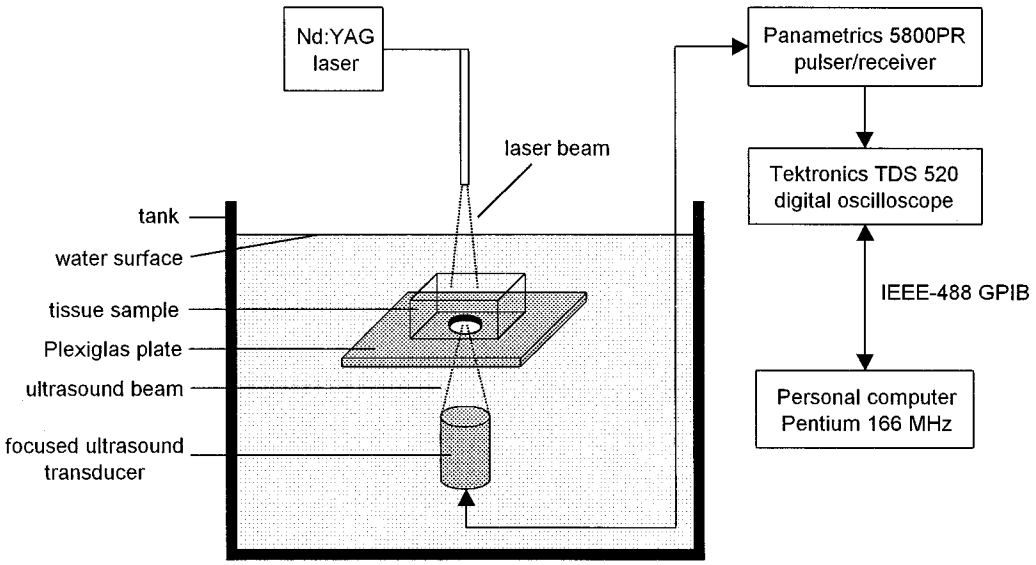

Fig. 1. Experimental setup and data acquisition system.

saline water. The Plexiglas plate had a 3-cm-diameter circular hole in the center. To prevent the tissue from sinking into the hole, the hole was covered with a stainless steel screen of 5-mm meshes. The screen cords were 0.15 mm in diameter. To keep the tissue from floating, it was fixed on the plate with a rubber band on each of its four sides.

Nd : YAG laser radiation (wavelength 1064 nm, TRIMEDYNE OPTILASE 1000 Modified 90 W) delivered via a 600-μ-diameter optical fiber was used to heat the tissue. Before heating, the efficiency of the laser irradiation system was calibrated with a power meter, which allowed for the conversion of the power reading displayed on the laser control panel to the actual power delivered by the fiber to the tissue.

A Panametrics 10-MHz broadband single-element spherical focused ultrasound transducer was used. The diameter of the transducer was 13 mm, and the focal length was 70 mm. The -6-dB focal zone of the transducer, computed based on the manufacturer specifications, was 0.85 mm wide and 32 mm long. The transducer was placed face up at 61-mm beneath the tissue sample so that the acoustic beam focused inside the tissue. The transducer and the Plexiglas plate were arranged in such a way that the transducer beam axis vertically passed the center of the circular hole of the plate. The hole was large enough to allow the focused ultrasound beam to completely pass to the tissue without being obscured by the plate. The transducer was driven by a Panametrics 5800PR pulser/receiver. The pulse repetition rate of the pulser/receiver was set to 1 kHz. The echo signal received by the pulser/receiver was sent to and then digitized at 250 MHz by a Tektronics TDS 520 digital oscilloscope. To improve the signal-to-noise ratio, the ten most recently acquired digitized echo signals were averaged in the oscilloscope. Since the averaging could suppress information about the waveform change we were looking for in the echo signals, averaging over a larger number of signal samples was avoided. The averaged digitized signals were then sent to a Pentium 166-MHz PC through an IEEE-488 GPIB board. The signal acquisition was computer-controlled via a LabView program developed at the laboratory, and was carried out automatically every 5 s.

Before laser irradiation, the ultrasound speed in the tissue sample was measured using the method presented in [3]. After laser irradiation, we could see a circular tissue surface area bleached by the laser heating. Since optic beam spot was adjusted to be concentric with the ultrasound beam axis, the bleached circular area was also concentric with the ultrasound beam axis during the heating. We cut the tissue sample into two parts along a vertical plane passing the center of the bleached surface area. This was a plane in which the ultrasound beam was lying during laser heating. We could see an area of pallor caused by laser heating, surrounded by nonirradiated tissue in dark red color. We regarded the boundary of this pale area as the coagulation front and measured the vertical distance from the center of the bleached circular tissue surface area to the front of the coagulated region. This distance was used as the tissue coagulation depth. Then we cut off a slice of tissue (about 2 mm thick), and took its picture.

III. Echo-Tracking Technique Utilized in this Investigation

The purpose of the echo tracking was to identify the portion of an echo signal returned from a predetermined tissue region during heating. First we applied many time windows to the first echo signal. The number of the windows depended on their distance and the length of the signal. Let τ_s be the length of the transmitted ultrasonic pulse, τ_w the width of each time window, and $t_0[i]$ the beginning of the ith time window ($i = 1, 2, \ldots, N$) with the subscript "0" denoting the value obtained prior to heating. Let $t_{\rm ref}$ be the round-trip transit time for acoustic waves to travel between the transducer and tissue surface facing the transducer (see Fig. 2 for notations). The echo signal covered by the ith window is the contribution of scattering from a portion of tissue delimited by $za_0[i]$ and $zb_0[i]$ (Fig. 2)

$$za_0[i] = \begin{cases} 0, & \text{if } 0 \le t_0[i] - t_{\rm ref} \le \tau_s \\ c_0 \times (t_0[i] - t_{\rm ref} - \tau_s)/2, & \text{if } t_0[i] - t_{\rm ref} > \tau_s \end{cases} \tag{1}$$

$$zb_0[i] = c_0 \times (t_0[i] - t_{\rm ref} + \tau_w)/2 \tag{2}$$

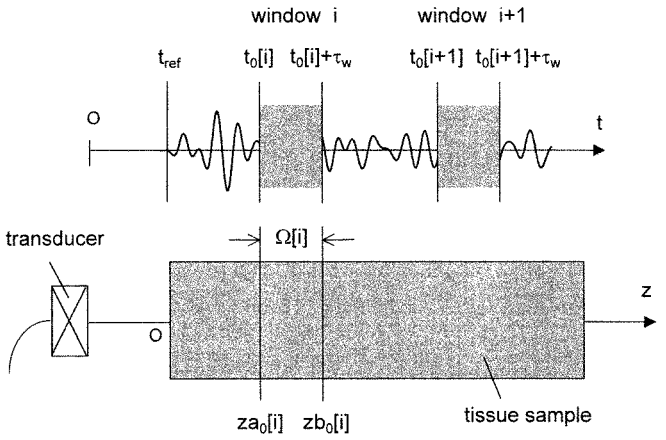

Fig. 2. Coordinate systems used throughout this paper and notations used in (1) and (2).

where c_0 is the initial ultrasound speed in the tissue sample prior to laser irradiation and measured using the method presented in [3]. In this study, $\tau_s = 0.4$ μs, the value of τ_w was set to $\tau_w = 8/f_c = 1.14$ μs, where $f_c = 7$ MHz was approximately the center frequency of the echo signal. In order to gain more spatial information, the distance between the beginning moments of two neighboring windows was set to 0.45 τ_w, i.e., the time windows overlapped each other by 45% of their width.

Let $\Omega[i]$ be the portion of tissue (or group of tissue scatters) initially delimited by $za_0[i]$ and $zb_0[i]$, and $\rho[i]$ the cross-correlation function between the signals contributed solely by $\Omega[i]$ and acquired during the current and last signal acquisitions. The value of $\rho[i]$ was computed using exactly the same echo tracking approach and parameters settings as those in [3]. Readers are referred to [3] for details.

IV. Quantitative Descriptions of Waveform Change and Their Use in Representing the Spatial Profile of Tissue Coagulation Damage

We define the following parameter as a measure of entire waveform change of the current signal with respect to the last one:

$$\beta = 1 - \frac{1}{N}\sum_{i=1}^{N}\rho[i] \tag{3}$$

where N is the total number of time windows, which varied between 24 and 57 depending on tissue thickness.

We define another parameter to quantitatively describe the waveform change of the current signal, $S_{\text{curr}}[i]$, which was scattered from $\Omega[i]$, with respect to a reference signal, $S_{\text{ref}}[i]$, which was scattered some moment ago from the same tissue region $\Omega[i]$. Let $\rho_{\text{ref}}[i]$ be the correlation coefficient between $S_{\text{curr}}[i]$ and $S_{\text{ref}}[i]$. The second parameter is defined as

$$\beta_{\text{ref}}[i] = \begin{cases} 1 - \dfrac{1}{M}\displaystyle\sum_{j=i-M+1}^{i}\rho_{\text{ref}}[j], & \text{if } M \le i \le N \\ 1 - \dfrac{1}{i}\displaystyle\sum_{j=1}^{i}\rho_{\text{ref}}[j], & \text{if } 1 \le i < M \end{cases} \tag{4}$$

where M is the number of time windows over which the mean of $\rho_{\text{ref}}[i]$ is computed. Due to the complexity of tissue structure change during heating, the value of $\rho_{\text{ref}}[i]$ may fluctuate significantly with gate position. In order to capture the general trend in signal waveform change without being misled by its local behavior, a spatially averaged value of $\rho_{\text{ref}}[i]$ is used in the definition of $\beta_{\text{ref}}[i]$ in (4). In our work, $M = 5$ was used for the spatial averaging.

The parameter β is an averaged value of $1-\rho[i]$ over all the time windows. It provides a way to determine how fast the entire signal is changing during heating. A larger value of β indicates a more significant signal change. If the signal has not changed, $\rho[i] = 1$, and hence $\beta = 0$. The same is true for $\beta_{\text{ref}}[i]$. However, $\beta_{\text{ref}}[i]$ tells how much the signal waveform has changed with respect to a reference signal and this for a particular region of interest.

Both changes in tissue temperature and structure can result in signal waveform change. Since our goal was to determine the tissue structure change, we needed to minimize the effect of temperature change while using the signal waveform-change information. This was achieved by selecting an appropriate reference signal. According to the current understanding of laser-tissue interaction, when subject to coagulative heating, the tissue goes through three major phases [1]. In the first phase, the tissue temperature increases rapidly. Afterwards, the tissue temperature quickly approaches an equilibrium and the tissue goes through a transition phase. Then the tissue thermal coagulation occurs as the heating continues. Through our study in [3], we found that the first phase may be identified by a large peak of β immediately upon the application of laser irradiation [see Fig. 3(a)], the second phase by a drop of β value following this large peak, and the third phase by a second rising of β value. Note that patterns similar to that shown in Fig. 3(a) occurred in all the experiments.

Based on the above analysis, we decided to choose a signal acquired during the second phase of coagulative heating, which was characterized by a quick drop of β value following the first large peak, as reference signal. In this way, we avoided the effect of the fast temperature change appeared during the first phase of coagulative heating. Specifically, we chose the echo signal acquired at 10 s following the first peak value of β as the reference signal, assuming that at this moment, the tissue temperature had already reached an equilibrium and that beyond this point the signal waveform change was mainly caused by the irreversible change of tissue structure.

Once the spatial profile of signal waveform change, characterized by the parameter $\beta_{\text{ref}}[i]$, was computed, we interpolated the computed result in both spatial and temporal dimensions to enhance the resolutions in both dimensions for better display. Thirty points were inserted between every pair of neighboring points in each of the two dimensions, and a linear interpolation algorithm was employed. We regarded the 2-D image of the interpolated result as the spatial profile of the degree of tissue coagulation damage in this study.

V. Evaluation of the Technique

To assess the correctness of the spatial profile of tissue coagulation damage computed by our technique, we used two qualitative but direct approaches and one quantitative but indirect approach. The first qualitative approach was intuitive: we directly

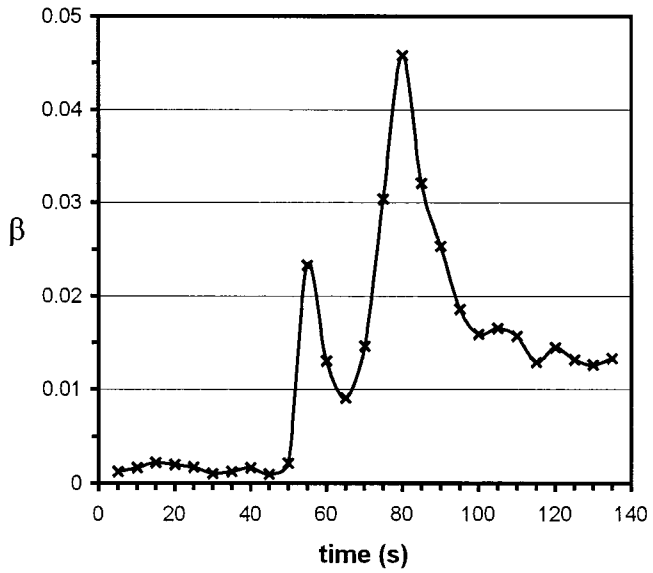

(a)

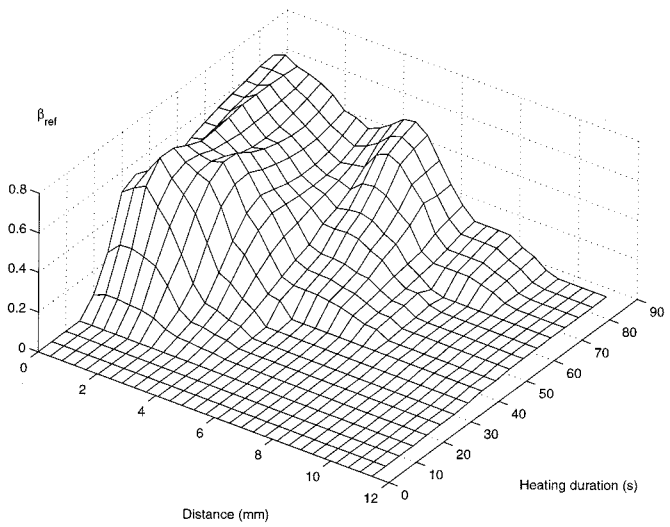

(b)

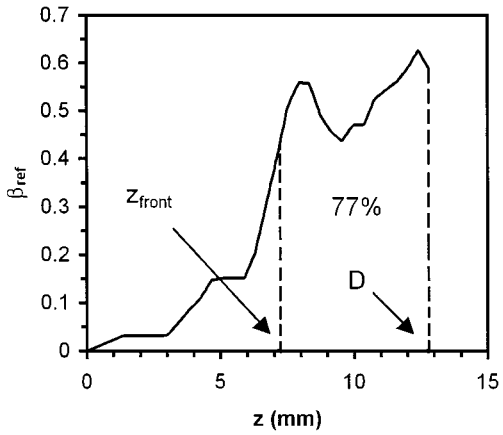

(c)

Fig. 3. (a) The value of β [cf. (3)] computed based on the echo signals acquired during laser irradiation in experiment #20. Signal acquisition began at 0 s and echo signals were acquired every 5 s. Laser was applied to the tissue at 50 s into the signal acquisition. We consider that the coagulation began at 65 s into the data acquisition, i.e., at 15 s into the heating. (b) Temporal and spatial variations of $\beta_{\rm ref}$ [cf. (4)] during heating. The results were computed based on the echo signals acquired during laser irradiation in experiment #20. Coagulation was considered to begin at 15 s into the heating. Before this moment, the values of $\beta_{\rm ref}$ were set to zero. The distance shown is the distance from the tissue sample surface facing the laser to a point inside the tissue and on the beam path of ultrasonic waves. One can see the expansion of larger valued $\beta_{\rm ref}$ during heating. (c) The position of coagulation front as determined by the method presented in Section V is indicated by $z_{\rm front}$. The values of $\beta_{\rm ref}$ [see (4)] were computed at 85 s into the heating, and based on the echo signals acquired in experiment #20. In computing $z_{\rm front}$, the value of γ_2 was set to 0.77; this means that beyond $z_{\rm front}$, the area beneath curve $\beta_{\rm ref}$ counts for 77% of the total area beneath this curve. The tissue thickness is denoted by D.

compared the spatial profile, displayed in the 2-D image, with visually inspected actual tissue damage. The second qualitative approach was to check the consistence of the damage pattern in the computed profile with the existing theoretical and experimental findings in the literature on the laser-tissue interaction. The third approach was quantitative but indirect, in which we used the computed spatial profile of tissue damage to calculate the coagulation depth. We compared the computed final coagulation depth with the actual coagulation depth as determined by visual inspection.

Let us first look at one of the experimental results shown in Fig. 3(b), which shows the variation of $\beta_{\rm ref}$ as a function of heating duration and location inside the tissue. One can see the progress of the region with large $\beta_{\rm ref}$ values along with heating. We consider this an indication that tissue coagulation is taking place and progressing. The boundary of this region should be related to the coagulation front. After carefully analyzing all our experimental data, we developed a procedure, described below, to correlate the boundary of the region with large $\beta_{\rm ref}$ values to the front of coagulated region.

The key components of the procedure were two thresholds. The first one, denoted by γ_1 ($0 \leq \gamma_1 \leq 1$), was used to determine whether the tissue (or signal) change was big enough for us to determine the coagulation front. To determine the appropriate value of γ_1, we acquired ten signals before the laser was turned on and computed $\rho[i]$ between each pair of two echo signals acquired consecutively. Since no heating had been applied yet, the signal waveform change was only caused by noise. Let $\rho_m[i]$ ($m = 1, 2, \ldots, 9$) be the correlation coefficient between the mth and $(m+1)$th echo signals acquired at gate i. We com-

puted the value of the following parameter and used it as a measure of noise level at different gate positions:

$$\beta_{\text{noise}}[i] = \begin{cases} \max\left\{1 - \dfrac{1}{M}\displaystyle\sum_{j=i-M+1}^{i}\rho_m[j]\right\}, & \text{if } M \le i \le N \\ \max\left\{1 - \dfrac{1}{i}\displaystyle\sum_{j=1}^{i}\rho_m[j]\right\}, & \text{if } 1 \le i < M \end{cases} \quad m = 1, 2, \ldots, 9 \tag{5}$$

where $\max\{\cdot\}$ denotes the maximum of the nine computed values. The parameter M, defined in (4), was set to five in our case. After experimenting with different γ_1 values, we set

$$\gamma_1 = 0.03. \tag{6}$$

If at a given moment into the heating the following condition was met:

$$\max\{\beta_{\text{ref}}[i] - \beta_{\text{noise}}[i]\} + \min\{\beta_{\text{ref}}[i] - \beta_{\text{noise}}[i]\} \ge \gamma_1, \quad i = 1, 2, \ldots, N \tag{7}$$

where $\min\{\cdot\}$ denotes the minimum of all the values computed at N time gate positions, we considered that coagulation front was determinable and proceeded further. Otherwise, we simply considered that the tissue structure had not changed enough and that the coagulation depth was zero.

The second threshold, denoted by $\gamma_2 (0 < \gamma_2 < 1)$, was used to determine the boundary of the region with large β_{ref} values to match the position of the coagulation front. More precisely, the coagulation front position, denoted by z_{front}, was determined as the point beyond which the area below the curve β_{ref} equaled the product of γ_2 and the total area beneath the curve [see Fig. 3(c)]. In this study, the value of γ_2 was set to 0.77, which was experimentally found to be the optimal setting that generated the most accurate overall estimations of final coagulation depths in comparison with visually inspected results in the sense of least mean squares.

The last stage of the procedure was to use a weighted moving averaging method for data-smoothing. We found that the following formula produced quite satisfactory results:

$$d_{\text{curr}} = \begin{cases} d_{\text{front}}, \\ \quad \text{if } d_{\text{last}} = 0 \\ 0.5d_{\text{front}} + 0.5d_{\text{last}}, \\ \quad \text{if } d_{\text{bflast}} = 0 \text{ and } d_{\text{last}} > 0 \\ 0.5d_{\text{front}} + 0.25d_{\text{last}} + 0.25d_{\text{bflast}} \\ \quad \text{if } d_{\text{bflast}} > 0 \text{ and } d_{\text{last}} > 0 \end{cases} \tag{8}$$

where $d_{\text{front}} = D - z_{\text{front}}$, with D being the tissue thickness, represents the coagulation front position as determined using the threshold method [cf. Fig. 3(c)]. In (8), d_{last} and d_{bflast} denote respectively the estimated depths of coagulation front positions at the moments of the last signal acquisition and the one before.

VI. Results

We carried out 23 laser experiments. Fig. 4 shows an image of the computed spatial profile, along the ultrasound beam axis, of tissue coagulation damage obtained from experiment #18. The horizontal axis represents the distance from the tissue surface facing the laser to a point inside the tissue that is located along the ultrasound beam path. The vertical axis represents heating duration. Fig. 5 shows a picture of a slice of irradiated tissue sample from experiment #18, whose computed spatial profile of coagulation damage is displayed in Fig. 4. The coagulated region is the pallor area on the left edge of the tissue. The picture captured the tissue damage status at the end of heating, which lasted 40 s in the experiment. Figs. 4 and 5 should be compared at 40 s into the heating and for the tissue region that was on the acoustic beam axis during the heating.

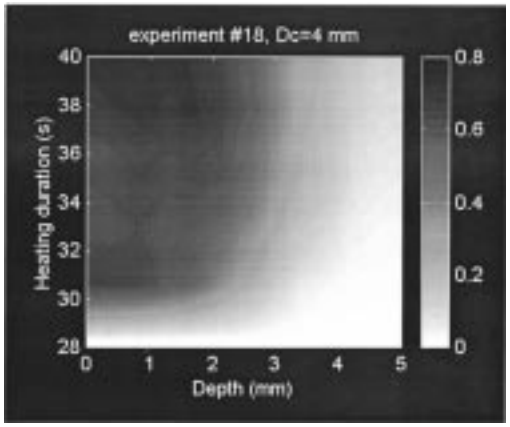

Fig. 4. Image representation of the spatial and temporal variation of β_{ref} [cf. (4)] during heating in experiment #18. On the gray level scale, the larger value corresponds to bigger signal waveform change. The distance shown is the distance from the tissue sample surface facing the laser to a point inside the tissue and on the beam path of the ultrasound transducer. The final visually inspected coagulation depth, denoted by D_c, is also given in the figure.

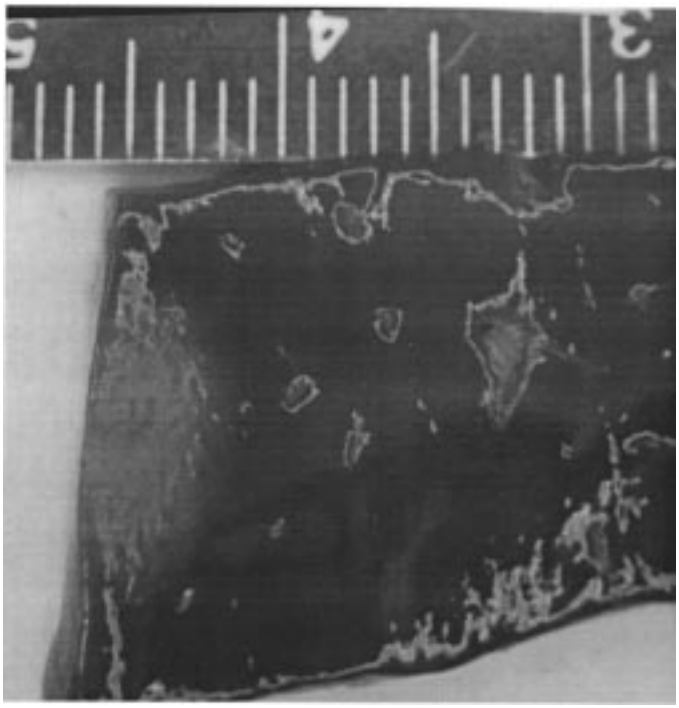

Fig. 5. Picture of a slice of the irradiated tissue sample in experiment #18.

The conditions of all the 23 experiments are listed in Table I. The ultrasonically detected final positions of the coagulation fronts for these experiments are also given in Table I, together with the corresponding visual inspection results and the measured speeds of sound in the tissue samples. The rms difference

TABLE I
CONDITIONS AND RESULTS FOR 23 LASER HEATING EXPERIMENTS

Experiment number	Effective light intensity (W/cm^2)	Heating duration (s)	Thickness of tissue sample (mm)	Measured speed of sound (m/s)	Final coagulation depth (mm)	
					Visual examination	Ultrasound estimation
1	62.6	45	18.33	1573.8	4	2.5
2	62.6	45	14.48	1584.7	3.5	5.3
3	62.6	45	22.78	1426.8	4	4.1
4	62.6	45	17.86	1570.9	4	3.9
5	62.6	85	15.53	1573.7	5	3.4
6	62.6	85	17.79	1587.3	4	3.9
7	62.6	85	29.19	1585.0	4.5	4.5
8	62.6	85	20.78	1572.7	5	4.8
9	62.6	235	20.61	1574.9	6	5.4
10	62.6	350	20.58	1575.0	6	5.1
11	83.5	20	11.05	1569.0	3	3.5
12	83.5	20	22.89	1423.7	3	3.0
13	83.5	20	20.04	1579.1	3	2.0
14	83.5	20	18.04	1567.5	3	1.9
15	83.5	35	12.97	1571.5	4	3.2
16	83.5	35	21.59	1585.4	4	3.9
17	83.5	35	22.87	1573.7	4.5	5.0
18	83.5	40	19.08	1625.7	4	2.8
19	83.5	45	23.00	1576.6	5	4.7
20	83.5	85	12.82	1568.7	6	5.1
21	83.5	120	15.59	1563.9	7	7.2
22	104.4	20	22.19	1582.2	3	3.2
23	104.4	35	24.39	1576.9	4	3.9

between ultrasonically determined and visually inspected coagulation depths was 0.81 mm.

VII. DISCUSSION

Comparing the spatial profile image of experiment #18, shown in Fig. 4, with the corresponding picture of the irradiated tissue sample in Fig. 5, one sees that the computed spatial profile is in qualitative accord with that of actual tissue damage. The computed spatial profile shows that the most severely coagulated region, as indicated by the darker color, ranges from about 1 to 2 mm at 40 s into the heating (the time the laser was turned off). This is consistent with the most damaged region shown in the corresponding picture as evidenced by the darker area in the middle of the coagulated region. These direct comparison results alone, though qualitative, have demonstrated, to a certain extent, the effectiveness of our technique.

Now let us use the second qualitative evaluation approach. Through the image in Fig. 4 one can see the progress of tissue damage, which is represented by large β_{ref} values, along with heating. The damaged tissue region progresses with time, first rather quickly and then markedly more slowly, which is consistent with the existing theoretical and experimental findings on the relationship between the advance of coagulation and heating duration in the literature [1]. One can also observe that the degree of coagulation damage varies with location inside the tissue. The most severely coagulated region ranges from about 1 to 2 mm below the tissue surface facing the laser. This is consistent with the post-experiment examination results of the heated tissue samples. We found that the most deeply coagulated tissue region was not situated on the tissue surface that was directly irradiated upon, but was about 1 to 2 mm deeper. There are two physical reasons responsible for this phenomenon [1]. On the one hand, the heat produced by optical absorption on the surface area of the tissue quickly dissipated into the surrounding cool water such that the tissue temperature on the surface was lower than that of subsurface tissue during the heating. On the other hand, it has been shown [1] that for infrared radiation, when laser beam impinges from water on an optically heterogeneous tissue, owing to the combined effects of multiple optical scattering inside the tissue and optical reflection at tissue-water interface, the maximum deposition of optical radiation is not on the tissue surface but at a depth of about 1 to 2 mm.

Finally, let us look at the overall outcome of using the quantitative evaluation approach. For the 23 experiments, good agreement with a rms difference of only 0.81 mm was obtained between the computed and visually inspected final coagulation depths.

Qualitative and quantitative assessments of the technique suggest that the waveform change parameter defined in (4) could

be used to reasonably represent the spatial profile of the degree of tissue coagulation damage. However, (4) is not the only way to describe waveform change, and there are other ways to define the change on the basis of the cross-correlation coefficient. Further studies are needed to address the following issues. First, the coagulation depth obtained directly from the curve β_{ref}, i.e., $d_{\text{front}} = D - z_{\text{front}}$, is not accurate, which is why the data-smoothing process represented by (8) is used. Physically the coagulation depth is determined by the entire history of heating (i.e., the accumulative effect of heating) and as a consequence, the current coagulation depth should relate to the previous one in some way. The data-smoothing process of (8) is just one way. However, it is possible to avoid the data-smoothing process if a more appropriate parameter similar to β_{ref} can be found and used. Second, the parameter defined in (4) has a very limited dynamic range. No matter how significant the signal waveform change is, the value of this parameter will not exceed one. For this reason, the laser intensity in our study was relatively low so that the signal waveform change could be reasonably well represented by this parameter without saturation. New parameters with larger dynamic representation ranges need to be found. Third, the parameter β_{ref} shows the spatial profile of thermal damage only in a relative sense. It remains a major challenge to find a parameter whose value can be used to indicate absolute degree of thermal damage.

The technique presented in the paper is phase sensitive. It has the same limits as that presented in [3]. It should also be pointed out that in this feasibility study the laser fiber and ultrasound transducer were placed on the two sides of the tissue (but they do not have to be collinear). This kind of setup reduces the value of the technique for clinical applications. It is necessary to investigate other configurations in which laser source and ultrasound transducer can be placed on the same side of the tissue. One possibility is the use of a mono-element transducer with an hole in the middle for the insertion of the optical fiber.

VIII. Conclusion

We have developed a technique that uses the spatial profile of waveform change to represent the spatial profile of coagulative tissue damage during heating. Preliminary study based on 23 laser heating experiments on canine liver has shown promising results. The spatial profiles of the degree of coagulation damage in the heated tissues, as determined by our technique, qualitatively agreed with the grossly inspected results. They also appeared to be consistent with the experimental and theoretical findings in the literature on laser-tissue interaction. Moreover, we developed an automatic procedure to compute the coagulation depth using the spatial profiles of the waveform change. We used the result as an indirect but quantitative means for evaluating the technique. Good overall agreement with a rms difference of only 0.81 mm was obtained between the computed and visually inspected final coagulation depths for the 23 experiments.

The signal processing involved in the technique is simple and can be implemented in real time. The technique has the potential for providing a convenient and cost-effective way of generating feedback signal for real-time control of tissue thermal coagulation damage.

Acknowledgment

The authors would like to thank B. Bell for his contribution in constructing part of the experimental apparatus.

References

[1] A. J. Welch and M. J. C. Van Gemert, *Optical-Thermal Response of Laser-Irradiated Tissue*. New York: Plenum Press, 1995.

[2] S. J. Childs, *Laser-Assisted Transurethral Resection of the Prostate (TURP)*. Baltimore, MD: Williams and Wilkins, 1993, ch. 4, pp. 21–32.

[3] Z. Sun, H. Ying, J. Lu, B. Bell, D. F. Cowan, and M. Motamedi, "Automatic ultrasound determination of thermal coagulation front during laser tissue heating," *IEEE Trans. Ultrason., Ferroelect., Freq. Cont.*, vol. 46, pp. 1134–1146, Sept. 1999.

Zhigang Sun received the B.S. degree in radio electronics in 1984 from Wuhan University, Wuhan, China, the Diplôme d'Etudes Approfondies in physical acoustics in 1988 from the University of Paris 6, Paris, France, and the Ph.D. degree in acoustics in 1993 from the National Institute of Applied Sciences of Lyon, Lyon, France.

He is currently a Research Officer with the Industrial Materials Institute of the National Research Council Canada. His research interests include biomedical ultrasound, industrial applications of ultrasound nondestructive testing, and acoustic signal processing.

Hao Ying (S'88–M'90–SM'97) received the B.S. and M.S. degrees in electrical engineering from Dong Hua University, Shanghai, China, in 1982 and 1984, respectively, and the Ph.D. degree in biomedical engineering from The University of Alabama at Birmingham, Birmingham, in 1990.

He was on the faculty of The University of Texas Medical Branch at Galveston. He is currently an Associate Professor at Department of Electrical and Computer Engineering, Wayne State University, Wayne, NE. He is also an Advisory Professor of Dong Hua University. He has published one research monograph/advanced textbook *Fuzzy Control and Modeling: Analytical Foundations and Applications* (Piscataway, NJ: IEEE Press, 2000), and 44 peer-reviewed journal papers. He is a Guest Editor for *Information Sciences, International Journal of Intelligent Control and Systems*, and *Acta Automatica Sinaca*. In 1994, he served as a Program Chair for *The International Joint Conference of North American Fuzzy Information Processing Society* (NAFIPS) Conference, *Industrial Fuzzy Control and Intelligent System Conference*, and NASA *Joint Technology Workshop on Neural Networks and Fuzzy Logic*. Additionally, he has served as the Publication Chair for the 2000 *IEEE International Conference on Fuzzy Systems* and as a Program Committee Member for many other international conferences.

Jialiang Lu (M'00) received the B.S. and M.S. degrees in electrical engineering from Zhejiang University, Hangzhou, China, in 1983 and 1986, respectively, and the Ph.D. degree in electrical engineering from University of Houston, Houston, TX, in 1999.

He worked in the Scientific Instrument Department of Zhejiang University as an Assistant Professor from 1986 to 1995. From 1996 to 1999, he was a Research and Teaching Fellow in the Electrical and Computer Engineering Department at University of Houston. He is currently a Senior Application Analyst at Halliburton Corp., Houston, TX. His research interests include intelligent control, fuzzy control, predictive control, adaptive control, neural networks, system modeling, distributed intelligent measurement and control instrument and system, DSP, embedded microprocessor system, database, telecommunication, and computer networks.